Inorganic Chemistry
Article
pubs.acs.org/IC

A Study on the Luminescence and Energy Transfer of Single-Phase and Color-Tunable $KCaY(PO_4)_2:Eu^{2+},Mn^{2+}$ Phosphor for Application in White-Light LEDs

Wei-Ren Liu,*[,†] Chien-Hao Huang,[‡] Chiao-Wen Yeh,[§] Jen-Ching Tsai,[∇] Yi-Chen Chiu,[‡] Yao-Tsung Yeh,[‡] and Ru-Shi Liu*[,§]

[†]Department of Chemical Engineering, R&D Center for Membrane Technology, Chung Yuan Christian University, Chung Li, Taiwan, Republic of China

[‡]Material and Chemical Research Laboratories, Industrial Technology Research Institute, Hsinchu 300, Taiwan, Republic of China

[§]Department of Chemistry, National Taiwan University, Taipei 106, Taiwan, Republic of China

[∇]Department of Materials Science and Engineering, National Tsing Hua University, Hsinchu, Taiwan, Republic of China

ABSTRACT: Novel single-phased white light-emitting $KCaY(PO_4)_2:Eu^{2+},Mn^{2+}$ phosphors for light-emitting diode (LED) applications were synthesized by conventional solid-state reaction. The emission hue could be controlled by tuning the Eu^{2+}/Mn^{2+} ratio via the energy transfer; the the emission hue of $KCaY(PO_4)_2:Eu^{2+},Mn^{2+}$ varied from blue (0.1853, 0.2627) to white-light (0.3350, 0.3203) and eventually to purple (0.3919, 0.2867). The mechanism of energy transfer from a sensitizer Eu^{2+} to an activator Mn^{2+} in $KCaY(PO_4)_2:Eu^{2+},Mn^{2+}$ phosphors was demonstrated to be an electric dipole−quadrupole interaction. Combining a NUV 405-nm chip and a white-emitting $KCaY(PO_4)_2:1\%Eu^{2+},4\%Mn^{2+}$ phosphor produced a white-light NUV LED, demonstrating CIE chromaticity coordinates of (0.314, 0.329) and a color temperature of 6507 K.

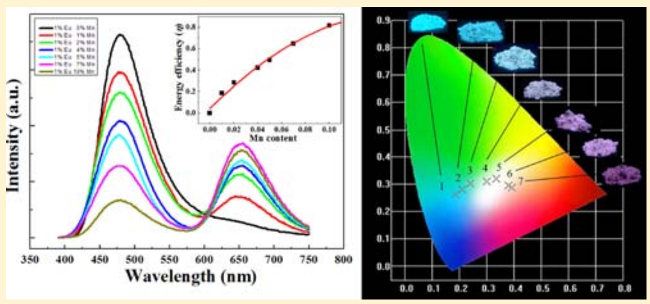

1. INTRODUCTION

In 1993, white light-emitting diodes (WLEDs) consisting of blue-emitting InGaN chip and yellow-emitting phosphor−$Y_3Al_5O_{12}:Ce^{3+}$ gave another revolution on the illumination to replace conventional incandescent or fluorescence lamps, because of the merits of being environmentally friendly and exhibiting energy savings, high brightness, and a long lifetime.[1,2] The drawbacks of the combination, however, are low color-rendering (*Ra* < 80), because of the scarcity of red emission, and different degradation rates of chip and phosphor, resulting in chromatic aberration and poor color stability for longer working times. For general lighting, a color rendering index of >85 is accepted.[3] For these reasons, single-composition white-emitting phosphors for ultraviolet (UV) or near-ultraviolet (NUV) excitations have been drawing much attention for solid-state lighting. Compared to the YAG-based system,[4] single-composition white phosphors with UV/NUV chips exhibit excellent *Ra* values and color stability. One of the strategies for generating white light from single-phased phosphors is by codoping sensitizer and activator into the same host. The energy transfer mechanism of sensitizer/activator, such as Eu^{2+}/Mn^{2+}, Ce^{3+}/Eu^{2+} and Ce^{3+}/Mn^{2+} have been investigated in many hosts, including $NaSr_4(BO_3)_3:Ce^{3+},Mn^{2+}$,[5] $NaBa_4(BO_3)_3:Ce^{3+},Mn^{2+}$,[6] $Sr_3B_2O_6:Ce^{3+},Eu^{2+}$,[7] and so on. Our preliminary research had published new single-phase phosphors, such as $Ca_{10}K(PO_4)_7:Eu^{2+},Mn^{2+}$, $Ca_9Y(PO_4)_7:Eu^{2+},Mn^{2+}$,[8] $Ca_9Y(PO_4)_7:Ce^{3+},Eu^{2+}$,[9] and $Ca_9Y(PO_4)_7:Ce^{3+},Mn^{2+}$,[10] for NUV LED applications. Wang et al.[11] reported the spectroscopic properties of red-emitting $KCaY(PO_4)_2:Eu^{3+}$ phosphors, peaking at 616 nm, excited in the vacuum ultraviolet (VUV) region. Zhang et al.[12] further investigated the VUV-UV spectroscopic properties of a series of RE (RE = Ce^{3+}, Eu^{3+}, and Tb^{3+})-doped $KMLn(PO_4)_2$ (M^{2+} = Ca, Sr; Ln^{3+} = Y, La, Lu) phosphors. To the best of our knowledge, the luminescence properties of $KCaY(PO_4)_2:Eu^{2+},Mn^{2+}$ (KCYP:Eu,Mn), as well as the mechanism of energy transfer and the fabrication for NUV LED, have not been reported in the literature.

Here, we report a novel emission-tunable white-emitting phosphor, $KCaY(PO_4)_2:Eu^{2+},Mn^{2+}$, in which the energy transfer mechanism between Eu^{2+} and Mn^{2+} in the host, as well as the luminescent properties and LED package, were first investigated in this study.

2. EXPERIMENTAL SECTION

2.1. Sample Preparation. Single-phase white-light phosphors $KCaY(PO_4)_2:1\%Eu^{2+},x\%Mn^{2+}$ were prepared via a conventional solid-state method. A series of $KCaY(PO_4)_2:1\%Eu^{2+},x\%Mn^{2+}$ phosphors was prepared from a mixture of K_2CO_3, $CaCO_3$, Y_2O_3, $(NH_4)_2HPO_4$,

Received: April 6, 2012
Published: August 24, 2012

Eu_2O_3, and MnO (all of which were analytical reagent (AR) grade) in the stoichiometric composition. The weighed powder was mixed in an agate mortar and placed in an alumina crucible. This crucible was heated at 1250 °C for 8 h under a reducing atmosphere of 15% H_2/85% N_2, and slowly cooled to room temperature.

2.2. Sample Characterization. The crystal structure and phase purity of $KCaY(PO_4)_2$:Eu^{2+},x%Mn^{2+} phosphors were carefully checked using powder X-ray diffraction (XRD) analysis (Bruker AXS D8) with Cu Kα radiation (λ = 1.5418 Å) planes collected within the 2θ range of 10°−80° at 45 kV and 40 mA. The photoluminescence (PL) and photoluminescence excitation (PLE) spectra were measured using a Spex Fluorolog-3 Spectrofluorometer (Instruments S.A., Edison, NJ, USA) equipped with a 450 W Xe light source and double-excitation monochromators. The samples were excited under 45° incidence, and emitted fluorescence was detected with a Hamamatsu Photonics R928 type photomultiplier perpendicular to the excitation beam. The CIE chromaticity coordinates for all samples were measured with a Laiko DT-101 color analyzer equipped with a CCD detector (Laiko Co., Tokyo, Japan).

3. RESULTS AND DISCUSSION

3.1. Crystal Structure. Figure 1 shows the XRD pattern of as-synthesized $KCaY(PO_4)_2$:Eu^{2+},Mn^{2+} phosphor, JCPDS standard pattern, and its crystal structure. All diffraction peaks of the as-synthesized sample were consistent with those of $KCaY(PO_4)_2$ (Joint Committee on Powder Diffraction Standards (JCPDS) File Card No. 51-1632). JCPDS reported the crystal structure to be hexagonal (space group $P6_222$) with lattice constants a = 6.903 Å, c = 6.331 Å, V = 261.26 $Å^3$, and Z = 1. The divalent ions occupied the large empty tunnels of the lattice and the trivalent position is statistically occupied by both Y^{3+} and Ca^{2+} ions. The structure of $KCaY(PO_4)_2$, shown in the inset of Figure 1, consists of chains of edge-sharing $(Ca,Y)O_8$ polyhedra interconnected by corner sharing. Our XRD results indicate that the structure of $KCaY(PO_4)_2$ host lattice were unchanged upon the doping of Eu^{2+} ions or the co-doping of Eu^{2+}/Mn^{2+}. The $KCaY(PO_4)_2$ has a hexagonal crystal structure with a space group of $P6_222$ (No. 161), similar to the structure of $KCaNd(PO_4)_2$,[13] which is composed of PO_4, CaO_8, YO_8, and KO_8 polyhedra in the lattice. The ionic radii for eight-coordinated Ca^{2+}, K^+, and Y^{3+} atoms are 1.15, 1.51, and 1.02 Å, respectively. The ionic radius of Eu^{2+} for eight-coordinated is 1.25 Å, while that for eight-coordinated Mn^{2+} is 0.96 Å. Thus, for the consideration of ionic radii matching, these Eu^{2+} and Mn^{2+} doping ions should occupy the Ca^{2+} or Y^{3+} ion sites in the $KCaY(PO_4)_2$ host.

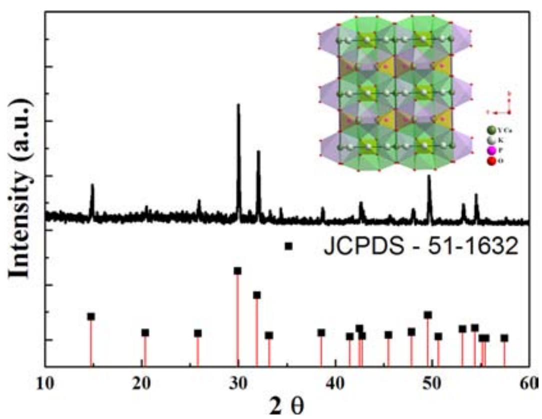

Figure 1. Powder XRD patterns of $KCaY(PO_4)_2$:1%Eu^{2+},1%Mn^{2+} and $KCaY(PO_4)_2$ standard pattern. The inset shows the crystal structure of $KCaY(PO_4)_2$.

3.2. Luminescence Properties. Figure 2 shows the reflectance spectra of the $KCaY(PO_4)_2$ host and the 1-mol %-Eu^{2+}-doped $KCaY(PO_4)_2$, respectively. The spectrum for $KCaY(PO_4)_2$ host exhibited an absorption band from 200 nm to 250 nm, which was due to the host absorption. Thus, the absorption edge of the $KCaY(PO_4)_2$ host could be determined to be 5.69 eV. While doping 1 mol % Eu^{2+} in the host, a strong and wide absorption band in the NUV range (270−500 nm) was observed, which mainly resulted from the transition of Eu^{2+} that originates from the $4f^7$ ground state to the $4f^6$ $5d^1$ excited state. Figure 3a further displays the PL/PLE spectra of the as-synthesized $KCaY(PO_4)_2$:1%Eu^{2+} phosphor. The inset in Figure 3a shows the PL intensity of $KCaY(PO_4)_2$ with different doping concentrations of Eu^{2+}. First of all, the PL spectrum of $KCaY(PO_4)_2$:1%Eu^{2+} exhibited a single blue emission peak at 480 nm, because of the 4f 5d transition of Eu^{2+} ions that occupy eight-coordinated Ca^{2+} sites in the lattice. The PLE spectrum of $KCaY(PO_4)_2$:1%Eu^{2+} shown in Figure 3a gives a broad hump between 250 nm and 450 nm, which is typically attributed to the 4f−5d electronic dipole-allowed transitions of Eu^{2+} with the electronic configuration of $4f^6$ $5d^1$. As shown in the inset of Figure 3a, the optimal doping concentration of Eu^{2+} in the $KCaY(PO_4)_2$ host is determined to be 5 mol %. The PL intensity decreased as long as the concentration exceeds the critical concentration, because of the phenomena of concentration quenching. As a result, the critical energy transfer distances between Eu^{2+} ions in the phosphor can be calculated by the following equation:[14]

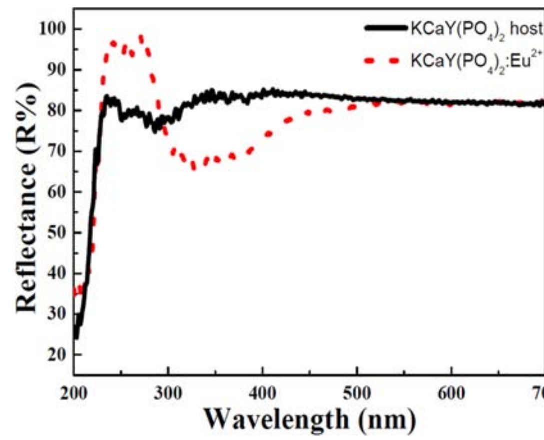

Figure 2. Reflectance spectra of the $KCaY(PO_4)_2$ host and the $KCaY(PO_4)_2$:1%Eu^{2+} phosphor.

$$R_c = 2\left[\frac{3V}{4\pi x_c Z}\right]^{1/3} \tag{1}$$

where x_c is the critical concentration, Z the number of cation sites in the unit cell, and V the volume of the unit cell. In this case, V = 261.26 $Å^3$, Z = 1, and the critical doping concentration of Eu^{2+} in the $KCaY(PO_4)_2$ host was determined to be 0.05. Thus, the R_c value of Eu^{2+} was then determined to be 21.53 Å.

To determine the absolute quantum efficiency of photoconversion for this phosphor, we applied the integrated sphere method for the measurements of optical absorbance (A) and quantum efficiency (Φ) of phosphor samples. The absorbance

dx.doi.org/10.1021/ic3007102 | Inorg. Chem. 2012, 51, 9636−9641

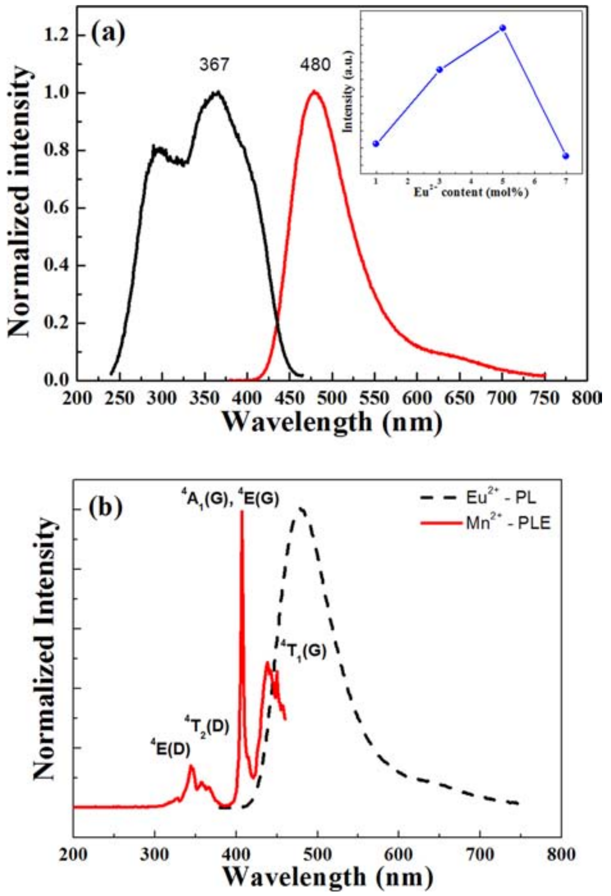

Figure 3. (a) Photoluminescence excitation/photoluminescence (PLE/PL) spectra of the as-synthesized $KCaY(PO_4)_2$:1%Eu^{2+} phosphor. The inset shows PL intensity of $KCaY(PO_4)_2$:Eu^{2+} phosphors as a function of Eu^{2+} concentration; (b) PLE spectrum of $KCaY(PO_4)_2$:1%Mn^{2+} and PL spectrum of $KCaY(PO_4)_2$:1%Eu^{2+}.

and quantum efficiencies of $KCaY(PO_4)_2$:1%Eu^{2+} phosphors can also be calculated using eqs 2 and 3:

$$A = \frac{L_o(\lambda) - L_i(\lambda)}{L_o(\lambda)} \quad (2)$$

where $L_o(\lambda)$ is the integrated excitation profile when the sample is diffusely illuminated by the integrated sphere's surface; $L_i(\lambda)$ is the integrated excitation profile when the sample is directly excited by the incident beam. Furthermore, the quantum efficiency (Φ) of $KCaY(PO_4)_2$:1%Eu^{2+} phosphors can be calculated by

$$\Phi = \frac{E_i(\lambda) - (1 - A)E_o(\lambda)}{L_e(\lambda)A} \quad (3)$$

where $E_i(\lambda)$ is the integrated luminescence of the powder upon direct excitation and $E_o(\lambda)$ is the integrated luminescence of the powder excited by indirect illumination from the sphere. The term $L_e(\lambda)$ is the integrated excitation profile obtained from the empty integrated sphere (without the sample present). The internal (η_i) and external (η_o) quantum efficiencies ($A \times \Phi$) were calculated based on the equations previously reported by Hirosaki et al.[15] The internal quantum efficiency of $KCaY(PO_4)_2$:1%Eu^{2+} and $BaMgAl_{10}O_{17}$:Eu^{2+} phosphor (commercial product KX661, from Kasei Optonix Ltd.) were found to be 35.8% and 93.8%, respectively, and the corresponding external quantum efficiencies are 21.4% and 71.9%, respectively, at the excitation wavelength of 365 nm. It is believed that the quantum efficiency of $KCaY(PO_4)_2$:Eu^{2+} phosphors could be further enhanced by tuning the synthetic conditions.

Figure 3b shows the excitation spectrum of $KCaY(PO_4)_2$:1% Mn^{2+} and the emission spectrum of $KCaY(PO_4)_2$:1%Eu^{2+}. As indicated in Figure 3b, with Mn^{2+} doping, the excitation peaks of $KCaY(PO_4)_2$:Mn^{2+} at 340, 355, 407, 418, and 469 nm were observed, corresponding to the transitions from the $^6A_1(^6S)$ to $^4E(^4D)$ (340 nm), $^4T_2(^4D)$ (355 nm), [$^4A_1(^4G)$, $^4E(^4G)$] (407 nm), $^4T_2(^4G)$ (418 nm), and $^4T_1(^4G)$ levels (469 nm) of Mn^{2+} luminescence center, respectively.[16] The observation of spectral overlap between the PL spectrum of $KCaY(PO_4)_2$:Eu^{2+} and the PLE spectrum of $KCaY(PO_4)_2$:Mn^{2+} indicates that the $KCaY(PO_4)_2$ host may undergo an energy transfer between the sensitizer Eu^{2+} ions and the activator Mn^{2+} ions.

3.3. Energy Transfer Mechanism of $KCaY(PO_4)_2$:Eu^{2+},Mn^{2+} Phosphors. Figure 4 shows the emission spectra of $KCaY(PO_4)_2$:1%Eu^{2+},x%Mn^{2+} phosphors (x = 0, 1, 2, 4, 5, 7, and 10) under 365-nm excitation. The inset in Figure 4 display the energy transfer efficiency with different Eu^{2+}/Mn^{2+} ratio in the $KCaY(PO_4)_2$ host. By co-doping Eu^{2+} and Mn^{2+} in the host, the phosphors generated blue and red emission bands, centered at 480 nm ($4f^6 5d^1 \rightarrow 4f^7$ transition of Eu^{2+}) and 652 nm ($^4T_1(^4G) \rightarrow {}^6A_1(^6S)$ transition of Mn^{2+}), respectively. The intensity of the Eu^{2+} blue emission at 480 nm decreased as the Mn^{2+} content increased to x. The intensity of the red emission at 652 nm increased as the Mn^{2+} content increased, reached a maximum at x = 7 mol %, and then decreased when x exceeded 7 mol %. The apparent decrease in the PL intensity for Mn^{2+} with $x > 7$ mol % is primarily due to the concentration quenching effect. The energy transfer efficiency of Eu^{2+} and Mn^{2+}, as a function of Mn^{2+} concentration, showed that the energy transfer efficiency increased as the Mn^{2+} concentration increased.

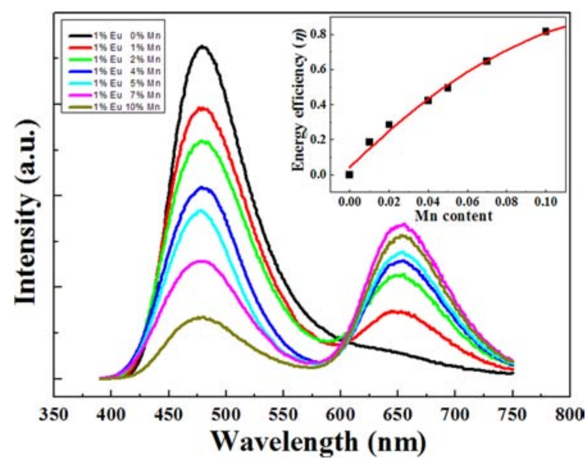

Figure 4. PL spectra of a series of $KCaY(PO_4)_2$:1%Eu^{2+},x%Mn^{2+} phosphors with different Mn^{2+} concentrations (x = 0, 1, 2, 4, 5, 7, and 10 mol %) excited at 365 nm. Inset shows the energy transfer efficiency Eu^{2+} to Mn^{2+}, as a function of Mn^{2+} content.

According to Dexter's energy transfer formula of multipolar interaction, the following relation can be obtained:[17]

$$\frac{I_{S0}}{I_S} \propto C^{\alpha/3} \quad (4)$$

dx.doi.org/10.1021/ic3007102 | Inorg. Chem. 2012, 51, 9636−9641

where I_{S0} and I_S are the luminescence intensities of the sensitizer Eu^{2+} with and without activator Mn^{2+} present, and C is then Mn^{2+} ion concentration. The plots of (I_{S0}/I_S) versus $C^{\alpha/3}$ with α = 6, 8, and 10 correspond to dipole−dipole, dipole−quadrupole, and quadrupole−quadrupole interactions, respectively. Figures 5a and 5b illustrate the relationships

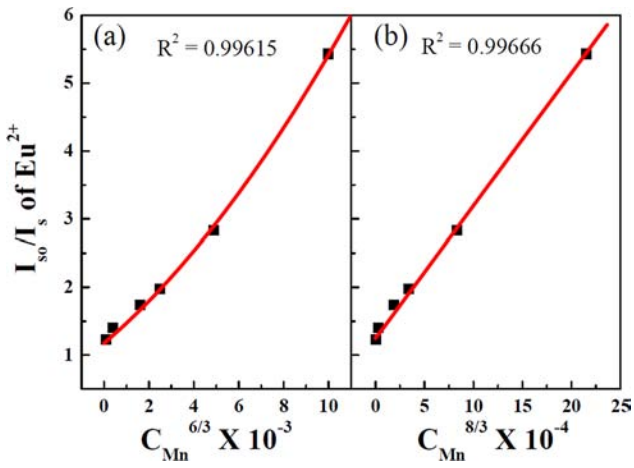

Figure 5. Dependence of I_{S0}/I_S of Eu^{2+} on (a) $C^{6/3}$ and (b) $C^{8/3}$.

between (I_{S0}/I_S) vs $C^{\alpha/3}$, revealing a linear behavior only when α = 8. Because of the fact that Mn^{2+} in phosphor is partial allowed, in most cases, the energy transfer is a quadrupole mechanism.[16,18] This implies that the energy transfer from the sensitizer Eu^{2+} to the activator Mn^{2+} follows a nonradiative dipole−quadrupole mechanism, which is similar to the results of previous reports.[19,20] Howwever, the similar linear curve for α = 6 might be due to the contribution of dipole−dipole energy transfer from Eu^{2+} ion to Eu^{2+} ion that resulted from the reabsorption phenomenon (as shown in Figure 3a).

Figure 6 and Table 1 provide a summary (in graphic and tabular form, respectively) of the CIE chromaticity of a single-phased emission-tunable phosphor $KCaY(PO_4)_2$:1%Eu^{2+},x% Mn^{2+} under 380 nm excitation (where x = 0, 1, 2, 4, 5, 7, and 10). The insets in Figure 6 also demonstrate the phosphor color images of different Eu^{2+}/Mn^{2+} molar ratios excited at 365 nm in an ultraviolet (UV) box. The chromaticity coordinates (x, y) were measured as (0.1853, 0.2627), (0.2107, 0.2796), (0.2399, 0.3032), (0.3001, 0.3102), (0.3350, 0.3203), (0.3810, 0.2951) eventually to (0.3919, 0.2867) for $KCaY(PO_4)_2$:1% Eu^{2+}, x%Mn^{2+} phosphors with x = 0, 1, 2, 4, 5, 7, and 10, respectively. These results indicate that changing the Mn^{2+} concentration can tune the color hue from blue (solely 1%Eu^{2+}, No. 1) through white light (1%Eu^{2+}/5%Mn^{2+}, No. 5) and eventually to red (1%Eu^{2+}/10%Mn^{2+}, No. 7) in the visible spectral region. Figure 7 show the decay lifetime of $KCaY(PO_4)_2$:1%Eu^{2+},x%Mn^{2+} phosphors (x = 0, 1, 2, 4, 5, and 7). The decay lifetime were fitted well by the Inokuti−Hirayama model[21] for Figures 7a and 7b. Based on the Inokuti−Hirayama model, the decay lifetimes of $KCaY(PO_4)_2$:Eu^{2+},Mn^{2+} are determined to be 0.46, 0.45, 0.43, 0.39, 0.21, and 0.18 μs for Mn concentrations of 0, 2, 4, 5, 7, and 10 mol %, with constant of 1% Eu, respectively, when monitored at 469 nm, as shown in Figure 7a. On the other hand, the decay lifetime of $KCaY(PO_4)_2$:Eu^{2+},Mn^{2+} for 0% Mn^{2+} to 7% Mn^{2+} with a constant of 1% Eu are all determined to be 0.06 ms when monitored at 655 nm, because of the energy transfer from Eu^{2+} to Mn^{2+}. The results indicate that Eu^{2+} and Mn^{2+} were substituted at a minimum of two different coordinated sites, which is consistent with our inference that the Eu^{2+} and Mn^{2+} sites should be occupied by Ca^{2+} and Y^{3+} ions, respectively, because of the consideration of ionic radii matching.

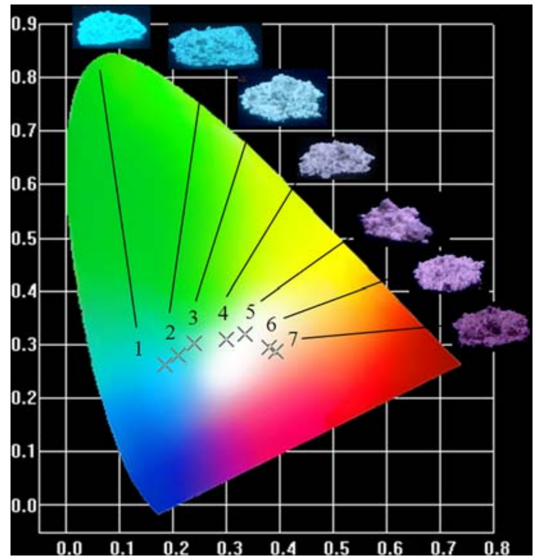

Figure 6. CIE coordinates of $KCaY(PO_4)_2$:1%Eu^{2+},x%Mn^{2+} phosphors (x = 0, 1, 2, 4, 5, 7, and 10). Numbers shown in the figure correspond to those described in Table 1. Insets show the phosphor images with different Mn^{2+} doping concentrations excited at 365 nm in the ultraviolet (UV) box.

Table 1. CIE Coordinates of $KCaY(PO_4)_2$:1%Eu^{2+},x%Mn^{2+} Phosphors (x = 0, 1, 2, 4, 5, 7, and 10) Excited at 380 nm

No.	composition	CIE (x, y)
1	$KCaY(PO_4)_2$:1%Eu	(0.1853, 0.2627)
2	$KCaY(PO_4)_2$:1%Eu,1%Mn	(0.2107, 0.2796)
3	$KCaY(PO_4)_2$:1%Eu,2%Mn	(0.2399, 0.3032)
4	$KCaY(PO_4)_2$:1%Eu,4%Mn	(0.3001, 0.3102)
5	$KCaY(PO_4)_2$:1%Eu,5%Mn	(0.3350, 0.3203)
6	$KCaY(PO_4)_2$:1%Eu,7%Mn	(0.3810, 0.2951)
7	$KCaY(PO_4)_2$:1%Eu,10%Mn	(0.3919, 0.2867)

3.4. Thermal Stability and LED Packages by NUV Chip.

For the application of high-powered LEDs, the thermal stability of phosphor is one of the important issues. Temperature dependence of luminescence for $KCaY(PO_4)_2$:Eu^{2+},Mn^{2+} under 380 nm excitation is shown in Figure 8. The activation energy (E_a) can be expressed by

$$\ln\left(\frac{I_o}{I}\right) = \ln A - \frac{E_a}{kT} \tag{5}$$

where I_o and I are the luminescence intensities of $KCaY(PO_4)_2$:Eu^{2+},Mn^{2+} phosphor (by integrating the area of each spectrum) at room temperature and the testing temperature, respectively; A is constant; and k is the Boltzmann constant (8.617×10^{-5} eV/K). The E_a value obtained was 0.025 eV. The inset of Figure 8 displays the thermal quenching of Eu^{2+} and Mn^{2+} emission intensity in $KCaY(PO_4)_2$ and Ce^{3+} emission in commercial YAG phosphor. The fair thermal stability, compared with YAG phosphor, demonstrated that $KCaY(PO_4)_2$:Eu^{2+},Mn^{2+} phosphor could be applied for high-powered LED applications.

dx.doi.org/10.1021/ic3007102 | Inorg. Chem. 2012, 51, 9636−9641

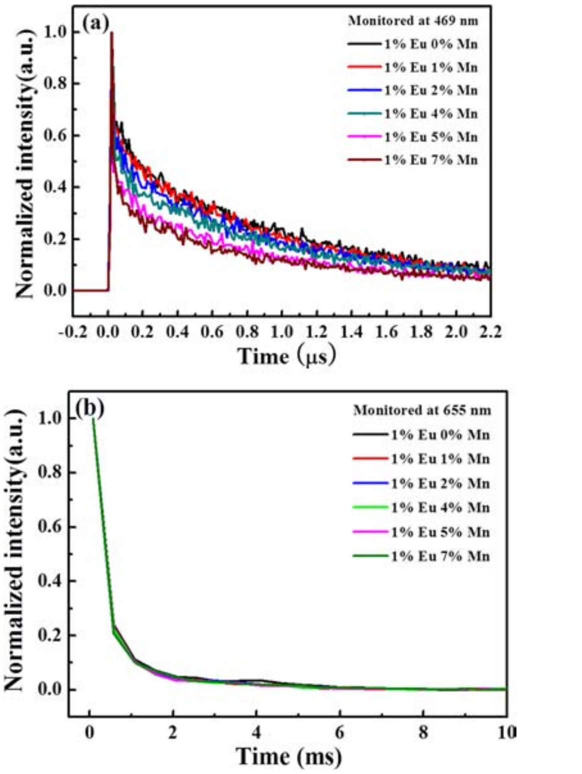

Figure 7. Decay lifetime tests of $KCaY(PO_4)_2$:1%Eu^{2+}, x%Mn^{2+} (x = 0, 1, 2, 4, 5, and 7) monitored at (a) 469 nm for Eu^{2+} emission and (b) 655 nm for Mn^{2+} emission.

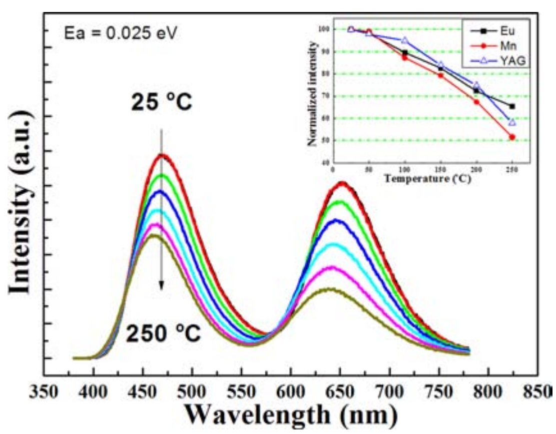

Figure 8. Temperature dependence of the PL intensity of $KCaY(PO_4)_2$:1%Eu^{2+}, 5%Mn^{2+} phosphor excited at 380 nm. The inset shows a plot of PL intensity versus temperature of the as-synthesized phosphor and commercial YAG phosphors.

Figure 9 shows the electroluminescent spectrum of white LED lamps fabricated using a NUV 405-nm chip combined with a single-phase white-emitting phosphor $KCaY(PO_4)_2$:1% Eu^{2+},4%Mn^{2+} driven by a 350 mA current. The inset displays the appearance of the NUV chip, in conjunction with $KCaY(PO_4)_2$:1%Eu^{2+},4%Mn^{2+} phosphor, after lighting with a 350 mA current. The white-light LED lamp package was fabricated by integrating a mixture of transparent silicone resin and white-emitting $KCaY(PO_4)_2$:1%Eu^{2+},4%Mn^{2+} phosphor dropped on a NUV 405-nm chip. The electroluminescent spectrum clearly shows three emission bands at 405, 490, and 652 nm, which are due to the NUV chip, Eu^{2+} emission, and

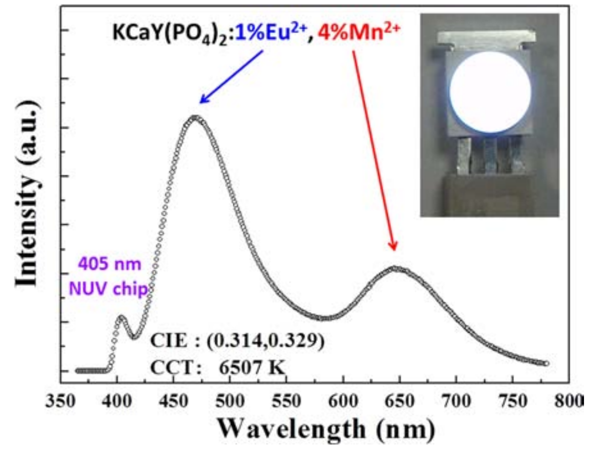

Figure 9. Electroluminescence spectra of white LED lamps fabricated using a NUV 405-nm chip combined with a white-emitting $KCaY(PO_4)_2$:1%Eu^{2+},4%Mn^{2+} phosphor driven by a current of 350 mA. Inset shows a photo of the LED package.

Mn^{2+} emission, respectively. The optical properties of the white-light LED, shown in Figure 9, gave a correlated color temperature of 6507 K and CIE color coordinates of (0.314, 0.329). The color rendering index values and the luminous efficacy of the fabricated white LED were 68.94 and 12.8 lm/W, respectively. The lower values of CRI and luminous efficacy were due to the apparent spectral deficiency in the green to yellow region and poor chip efficiency, which could be modified by adding green- and yellow-emitting phosphors and improving the chip efficiency. The inset of Figure 9 displays a photograph of the white-light LED lamp under a forward bias current of 350 mA. These results indicate that the composition-optimized $KCaY(PO_4)_2$:1%Eu^{2+},4%Mn^{2+} phosphor may have promising applications for white-light NUV LEDs.

4. CONCLUSIONS

This study reports the synthesis of novel single-phase white-light-emitting NUV LED phosphors $KCaY(PO_4)_2$:Eu^{2+},Mn^{2+}, using a solid-state reaction. The energy transfer from Eu^{2+} to Mn^{2+} in the $KCaY(PO_4)_2$ host was a resonant type, via a nonradiative dipole−quadrupole mechanism. A white light could be generated by NUV LED pumping by fabricating a NUV 405-nm chip to pump a single-phase white-light $KCaY(PO_4)_2$:1%Eu^{2+},4%Mn^{2+} phosphor driven by a current of 350 mA, producing a white light with a correlated color temperature of 6507 K and color coordinates of (0.314, 0.329). These results indicate that $KCaY(PO_4)_2$:Eu^{2+},Mn^{2+} is a promising single-composition phosphor for application involving white-light NUV LEDs.

■ AUTHOR INFORMATION

Corresponding Author

*Tel.:+ 886-3-2654140. E-mail: WRLiu@cycu.edu.tw (W.-R.L.), rsliu@ntu.edu.tw (R.-S.L.).

Notes

The authors declare no competing financial interest.

■ ACKNOWLEDGMENTS

This research was supported by Industrial Technology Research Institute (ITRI) (under Contract No. B301AR4Q40), the NSC (Contract No. 101-2218-E-033-

001), and the Economic Affair (Contract No. 97-EC-17-A-07-S1-043).

■ REFERENCES

(1) Uchida, Y.; Tagchi, T. *Opt. Eng.* **2005**, *44*, 124003.
(2) Nakamura, S.; Senoh, M.; Mukai, T. *Appl. Phys. Lett.* **1993**, *62*, 2390.
(3) Xie, R.-J.; Li, Y. Q.; Hirosaki, N.; Yamamoto, H. *Nitride Phosphors and Solid-State Lighting*; Taylor & Francis: Boca Raton, FL, 2011.
(4) Shimizu, Y.; Sakano, K.; Noguchi, Y.; Moriguchi, T. U.S. Patent No. 5,998,925, Dec. 7, 1999.
(5) Zhang, X. M.; Qiao, X. B.; Seo, H. J. *Curr. Appl. Phys.* **2011**, *11*, 442.
(6) Zhang, X. M.; Seo, H. J. *Physica B* **2010**, *405*, 2436.
(7) Chang, C. K.; Chen, T. M. *Appl. Phys. Lett.* **2007**, *91*, 081902.
(8) Huang, C. H.; Chen, T. M.; Liu, W. R.; Chiu, Y. C.; Yeh, Y. T.; Jang, S. M. *ACS Appl. Mater. Interfaces* **2010**, *1*, 259.
(9) Huang, C. H.; Luo, L. Y.; Chen, T. M. *J. Electrochem. Soc.* **2011**, *158*, J341.
(10) Huang, C. H.; Kao, T. W.; Chen, T. M. *ACS Appl. Mater. Interfaces* **2010**, *2*, 1395.
(11) Wang, D.; Wang, Y. *Mater. Sci. Eng., B* **2006**, *133*, 218.
(12) Zhang, Z. J.; Chen, S.; Wang, J.; Chen, H. H.; Yang, X. X. *Opt. Mater.* **2009**, *32*, 99.
(13) Vlasse, M.; Bochu, P.; Parent, C.; Chaminade, J. P.; Daoudi, A.; LeFlem, G.; Hagenmuller, P. *Acta Crystallogr., Sect. B: Struct. Sci.* **1982**, *38*, 2328.
(14) Blasse, G. *J. Solid State Chem.* **1986**, *62*, 207.
(15) Hirosaki, N.; Xie, R.-J.; Kimoto, K.; Sekiguchi, T.; Yamamoto, Y.; Suehiro, T.; Mitomo, M. *Appl. Phys. Lett.* **2005**, *86*, 211905.
(16) Yang, W. J.; Luo, L. Y.; Chen, T. M.; Wang, N. S. *Chem. Mater.* **2005**, *17*, 3883.
(17) Dexter, D. L.; Schulman, J. H. *J. Chem. Phys.* **1954**, *22*, 1603.
(18) Dexter, D. L. *J. Chem. Phys.* **1953**, *21*, 836.
(19) Jang, H. S.; Won, Y. H.; Jeon, D. Y. *Appl. Phys. B: Laser Opt.* **2009**, *95*, 715.
(20) Yang, W. J.; Chen, T. M. *Appl. Phys. Lett.* **2006**, *88*, 101903.
(21) Ross, J. B. A.; Schmidt, C. J.; Brand, L. *Biochemistry* **1981**, *20*, 4369.